Proc. Natl. Acad. Sci. USA
Vol. 96, pp. 1088–1093, February 1999
Neurobiology

Molecular and functional remodeling of electrogenic membrane of hypothalamic neurons in response to changes in their input

(electrogenesis/gene transcription/ion channels/sodium channels)

M. TANAKA*†‡, T. R. CUMMINS*†, K. ISHIKAWA*†, J. A. BLACK*†, Y. IBATA‡, AND S. G. WAXMAN*†§

*Department of Neurology, Yale University School of Medicine, New Haven, CT 06510; †Neuroscience Research Center, Veterans Affairs Medical Center, West Haven CT 06516; and ‡Department of Anatomy and Neurobiology, Kyoto Prefectural University of Medicine, Kyoto 602, Japan

Communicated by Dominick P. Purpura, Albert Einstein College of Medicine, Bronx, NY, December 11, 1998 (received for review September 28, 1998)

ABSTRACT **Neurons respond to stimuli by integrating generator and synaptic potentials and generating action potentials. However, whether the underlying electrogenic machinery within neurons itself changes, in response to alterations in input, is not known. To determine whether there are changes in Na^+ channel expression and function within neurons in response to altered input, we exposed magnocellular neurosecretory cells (MNCs) in the rat supraoptic nucleus to different osmotic milieus by salt-loading and studied Na^+ channel mRNA and protein, and Na^+ currents, in these cells. *In situ* hybridization demonstrated significantly increased mRNA levels for α-II, Na6, β1 and β2 Na^+ channel subunits, and immunohistochemistry/immunoblotting showed increased Na^+ channel protein after salt-loading. Using patch-clamp recordings to examine the deployment of functional Na^+ channels in the membranes of MNCs, we observed an increase in the amplitude of the transient Na^+ current after salt-loading and an even greater increase in amplitude and density of the persistent Na^+ current evoked at subthreshold potentials by slow ramp depolarizations. These results demonstrate that MNCs respond to salt-loading by selectively synthesizing additional, functional Na^+ channel subtypes whose deployment in the membrane changes its electrogenic properties. Thus, neurons may respond to changes in their input not only by producing different patterns of electrical activity, but also by remodeling the electrogenic machinery that underlies this activity.**

The nervous system responds to environmental stimuli with altered patterns of electrical activity that trigger physiological responses and behaviors that tend to protect the organism and/or help it adapt to its environment. The molecular and cellular mechanisms underlying these altered patterns of neuronal activity are not fully understood. They depend, in part, on the integration of generator potentials and excitatory and inhibitory postsynaptic potentials that impinge on neurons within the circuit under study. Whether the electrogenic machinery responsible for this signal integration within these neurons itself changes, however, in response to environmental changes is not well understood.

A model for studying the neuronal response to environmental changes is provided by the magnocellular neurosecretory cells (MNCs) in the supraoptic nucleus (SON), which send axons to the neurohypophysis and fire in bursts so as to release vasopressin in response to increases in plasma osmolality. Vasopressin release is a function of action potential frequency in these cells (1, 2) and firing frequency, in turn, is modulated by osmotic stimuli (3–5). Action potential activity in these cells is Na^+ dependent and tetrodotoxin (TTX) sensitive, indicating that it is mediated by Na^+ channels (6–9). While it is known that eight types of Na^+ channels, encoded by distinct genes, are expressed in neurons (10–17), the identity of the Na^+ channels in supraoptic MNCs is not known. Moreover, the basic mechanisms that lead to these environmentally triggered changes in firing pattern in supraoptic neurons have been only partially delineated. It is known that MNCs possess an intrinsic regenerative mechanism (6, 18, 19), which can be triggered by endogenous osmosensitivity mediated by mechanosensitive channels (20), providing an electrogenic cascade that can respond to changes in the environment. There is also evidence for synaptic activation of MNCs, which leads to their firing and release of vasopressin, after exposure of circumventricular neurons to osmotic stimulation (21). In the present report we demonstrate an additional, previously undescribed, response of these cells to changes in their input: molecular and functional remodeling by means of the increased expression of specific Na^+ channel α- and β-subunit genes and addition of additional functional Na^+ channels that alter the electrogenic properties of the cell membrane.

MATERIALS AND METHODS

Salt-Loading. Adult male Sprague—Dawley rats (200–220 g), housed under a 12-h–12-h dark–light cycle, were salt-loaded with 2% NaCl (ad libitum) in their drinking water and unlimited access to food, and they were sacrificed after 7 days. All experiments were approved by the institutional animal use and care committee. To confirm the extent of salt-loading, plasma osmotic pressure was measured (vapor pressure osmometer model 5500; Wescor, Logan, UT), demonstrating a significant ($P < 0.01$) increase in salt-loaded rats (321.5 ± 4.48 milliosmolar) compared with controls (292.4 ± 0.79 milliosmolar). Body weights were significantly ($P < 0.01$) lower in salted-loaded (194.3 ± 11.9 g) compared with control (248.4 ± 7.11 g) rats. Ten animals (five control and five salt-loading) each were used for *in situ* hybridization, SP20 immunocytochemistry, and immunoblot analysis. Six control and six salt-loaded rats were used for patch-clamp studies.

***In Situ* Hybridization.** Rats were anesthetized with ketamine/xylazine (40/2.5 mg/kg, i.p.) and perfused with 4% paraformaldehyde in 0.14 M phosphate buffer. Brains were postfixed overnight at 4°C and cryoprotected, and serial coronal sections (30 μm) of hypothalamus were cut and collected in 4× SSC. Sections, including the SON from the level of the preoptic area rostrally to the retrochiasmatic area caudally, were divided into six groups for detection of Na^+ channel mRNAs. Sections from control and salt-loaded groups were

The publication costs of this article were defrayed in part by page charge payment. This article must therefore be hereby marked "*advertisement*" in accordance with 18 U.S.C. §1734 solely to indicate this fact.

PNAS is available online at www.pnas.org.

Abbreviations: MNC, magnocellular neurosecretory cell; SON, supraoptic nucleus (nuclei); DIG, digoxigenin; TTX, tetrodotoxin.

§To whom reprint requests should be addressed at: Department of Neurology, LCI 707, Yale Medical School, 333 Cedar Street, New Haven, CT 06510. e-mail: stephen.waxman@yale.edu.

hybridized in the same chamber by a free-floating method (22). Sections were deproteinized with proteinase K (2.5 μg/ml) acetylated with 0.25% acetic anhydride and 0.1 M triethanolamine and were incubated in hybridization buffer (50% formamide/10% dextran sulfate/20 mM Tris·HCl, pH 7.5/5 mM EDTA/0.3 M NaCl/0.2% SDS/500 μg/ml yeast tRNA/1× Denhardt's solution/10 mM DTT), containing digoxigenin (DIG)-UTP-labeled Na^+ channel riboprobe (0.25 ng/μl) for 12 h at 60°C. After rinsing in 2× SSC/50% formamide and RNase solution in 0.5× SSC, sections were transferred into buffer 1 (100 mM Tris·HCl, pH 7.5/150 mM NaCl), incubated in alkaline phosphatase-labeled anti-DIG antibody (dilution, 1:500 in buffer 1) overnight at 4°C, and reacted in a chromogen solution containing 4-nitroblue tetrazolium chloride (NBT) and 5-bromo-4-chloro-3-indolyl phosphate (BCIP) in buffer (100 mM Tris·HCl, pH 9.5/10 mM NaCl/50 mM $MgCl_2$) for 4 h at room temperature.

DIG-labeled antisense and sense riboprobes for Na^+ channel α-subunits α-I (nucleotides 7385–7820, GenBank numbering), α-II (nucleotides 6807–7302), α-III (nucleotides 6325–6822), Na6 (nucleotides 6461–6761), and β-subunit β1 (nucleotides 457–790) and β2 (nucleotides 140–669) were synthesized from each cDNA as previously described by reverse transcription–PCR (11). Transcription was carried out with 120 units of appropriate RNA polymerase and 1 μg of linearized template in a reaction mixture containing buffer (1×), 0.35 mM DIG-11-UTP, 1 mM GTP, ATP, and CTP, 0.65 mM UTP, 10 mM DTT, and 10 units of RNase inhibitor (Boehringer Mannheim). Sense riboprobes yielded no signals on *in situ* hybridization.

For quantitation of hybridization signal, images were captured with a ComputerEyes/1024, version 1.07, capture board. Optical densities (ODs) of the circumscribed SON were obtained within the linear calibration range by using the NIH IMAGE program, calibrated with neutral density filters of 0.1, 0.3, and 0.6 OD, and fitted to a straight line. Background OD, measured in the lateral hypothalamic area surrounding the SON in each section, was subtracted from all signals.

For colocalization of vasopressin and oxytocin peptide and α Na6 mRNA (Fig. 1), control rats were perfused and fixed as described above. Coronal cryostat sections (10 μm) were incubated overnight at 4°C with a mixture of guinea pig anti-vasopressin (1:1500; Peninsula Lab Inc., USA) and rabbit anti-oxytocin (1:1000; Peninsula Laboratories) in 0.1 M phosphate-buffered saline (PBS), treated with diethyl pyrocarbonate to protect from RNase. Sections were rinsed twice in PBS and incubated with fluorescein isothiocyanate (FITC)-labeled goat anti-guinea pig IgG (1:250; Vector Laboratories) and Texas red-labeled goat anti-rabbit IgG (1:250; Vector Laboratories) in PBS for 3 h at room temperature. After rinsing in 0.1 M PBS, sections were mounted on poly(L-lysine)-coated slides coverslipped with Vectashield (Vector Laboratories), and examined and photographed with an epifluorescence microscope equipped with a double filter for FITC and Texas red fluorescence. Sections were subsequently processed for *in situ* hybridization as described above, using a DIG-labeled probe that recognizes Na^+ channel α-subunit Na6. In control experiments, FITC-positive neurons after incubation with anti-oxytocin serum and Texas red-positive neurons after incubation with anti-vasopressin serum were not detected.

Immunocytochemistry and Immunoblotting. Antibody SP20 was generated against a conserved region of rat brain sodium channel (residues 1106–1126 of sodium channel II (23). The affinity purification and specificity of SP20 have been previously described (23.).

Rats were perfused with 4% paraformaldehyde, and the brain and pituitary were removed and postfixed for 3 h. After immersion in 20% sucrose in 0.1 M PBS for 24 h, cryosections (25 μm) containing SON, median eminence, and pituitary neural lobe were cut. Sections were incubated in blocking solution (PBS containing 5% normal goat serum and 1% BSA) containing 0.1% Triton X-100 twice for 15 min at room temperature, incubated with antibody SP20 (1:50) in blocking solution overnight at 4°C, washed twice in PBS, and incubated overnight at 4°C with biotinylated anti-rabbit serum (1:1000, Vector Laboratories). Sections were then incubated in avidin-biotin-peroxidase complex (ABC) (1:1000, Vector Laboratories) for 2 h, exposed for 10 min to 0.015% 3,3′-diaminobenzidine·4HCl in 0.05 M Tris·HCl buffer containing 0.005% H_2O_2. Control experiments in which the primary antibody or secondary antibody was omitted showed no staining.

Immunoblotting was carried out on samples derived from the SON of single rats and from the pooled posterior pituitary lobes of two rats. Equal volumes of membrane protein from each group (≈10–40 μg) were added to reducing SDS sample buffer, incubated at 37°C for 30 min, separated by SDS/6% polyacrylamide gel electrophoresis, and electrotransferred onto poly(vinylidene difluoride) (PVDF) membrane. Membranes were blocked with 10% nonfat dry milk in Tris-buffered saline (100 mM Tris, pH 8.0/0.9% NaCl) containing 0.1% Tween-20, and then incubated overnight at 4°C with SP20 (1:100). Membranes were washed and incubated with alkaline phosphatase-conjugated goat anti-rabbit IgG secondary antibody (1:1000) for 2 h at room temperature. After a brief wash, immunoreactive bands were visualized with 0.38% 4-nitroblue tetrazolium chloride/0.19% 5-bromo-4-chloro-3-indolyl phosphate.

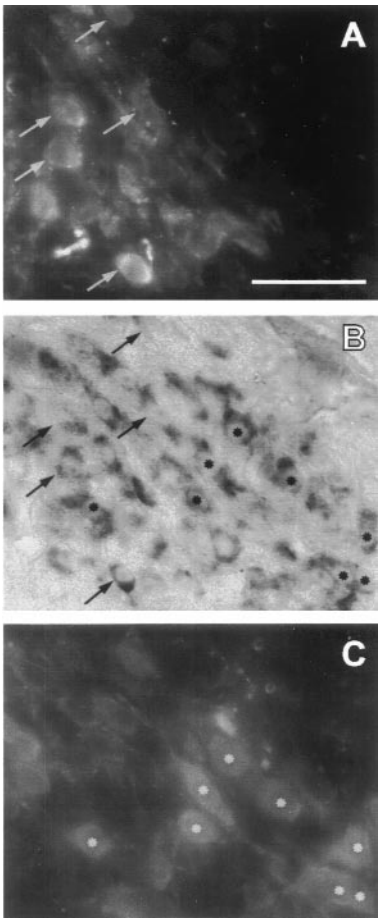

FIG. 1. *In situ* hybridization together with double immunofluorescence labeling demonstrates that mRNA for the Na6 sodium channel α-subunit (*B*) is present in both vasopressin-containing MNCs (*A*; same cells marked with arrows in *B*) and oxytocin-containing MNCs (*C*; same cells marked with asterisks in *B*) within the SON. (Bar = 50 μm.)

Membrane Preparations. SON and posterior lobe of the pituitary from control and salt-loading rats were quickly microdissected after decapitation, and crude lysed membrane fractions were prepared (24). In brief, 10- to 40-mg tissue samples were homogenized in 5 mM Tris·HCl, pH 7.4/0.3 M sucrose containing protease inhibitors (1 mM phenylmethanesulfonyl fluoride, 1 μg/ml leupeptin, and 2 μg/ml aprotinin), and nuclei and other debris were pelleted twice at 1,000 $\times$ *g* for 10 min. Supernatants were centrifuged at 350,000 $\times$ *g* for 5 min and resuspended in homogenization buffer. To obtain solubilized membrane fractions, 12.5% Triton X-100, 100 mM EDTA, and 2 M KCl were added to final concentrations of 2.5%, 2.5 mM, and 100 mM, and supernatants were incubated at 4°C for 1 h and then centrifuged at 16,000 $\times$ *g* for 10 min. Supernatants were used for protein quantitative analysis and immunoblot analysis. Protein was determined by using the D_c protein assay (Bio-Rad) with BSA as a standard.

Whole-Cell Patch Clamp. MNCs in the SON from adult male rats were dissociated as previously described (25) with modification. SON were dissected with iridectomy scissors in ice-chilled Ringer's solution without Ca^{2+}. They were transferred into complete saline solution (CSS; 137 mM NaCl/5.3 mM KCl/1 mM $MgCl_2$/25 mM sorbitol/10 mM Hepes, pH 7.2) supplemented with proteases X and XIV (1 mg/ml, Sigma), for 45 min at 23°C under oxygen bubbling and gentle stirring, rinsed in CSS for 15 min at 23°C under oxygen bubbling, and dissociated by mechanical trituration with graduated polished pipettes and placed on laminin-coated cover glasses in 35-mm Petri dishes. SON neurons were recorded in the whole-cell patch-clamp configuration within 2 h after dissociation. All recordings were made with an EPC-9 amplifier (v 7.52, HEKA Electronics, Lambrecht/Pfalz, Germany). Recording electrodes were 1–2 MΩ, and 80% series resistance compensation was used. The pipette solution contained 140 mM CsF, 2 mM $MgCl_2$, 1 mM EGTA, and 10 mM NaHepes, pH 7.3, and the extracellular solution contained 140 mM NaCl, 3 mM KCl, 2 mM $MgCl_2$, 1 mM $CaCl_2$, and 10 mM Hepes, pH 7.3. All recordings were conducted at room temperature (≈21°C).

RESULTS

We first investigated expression of mRNA encoding Na^+ channel α (I, II, III, Na6) and β (β1 and β2) subunits known to be present in the brain by *in situ* hybridization using isoform-specific riboprobes in adult rats under normal conditions and after chronic salt-loading, which exposes SON neurons to elevated extracellular osmolality (26–28).

Almost all MNCs in the SON displayed moderate levels of α-II and Na6 mRNA in control rats. Combining *in situ* hybridization with double immunofluorescence labeling, we observed that both vasopressin and oxytocin-containing MNCs of the SON express Na6 mRNA (Fig. 1). Significant levels of α-I and α-III mRNA could not be detected in MNCs. mRNAs for both Na^+ channel β subunits are present in MNCs, β1 at low-to-moderate levels and β2 at moderate levels (Fig. 2).

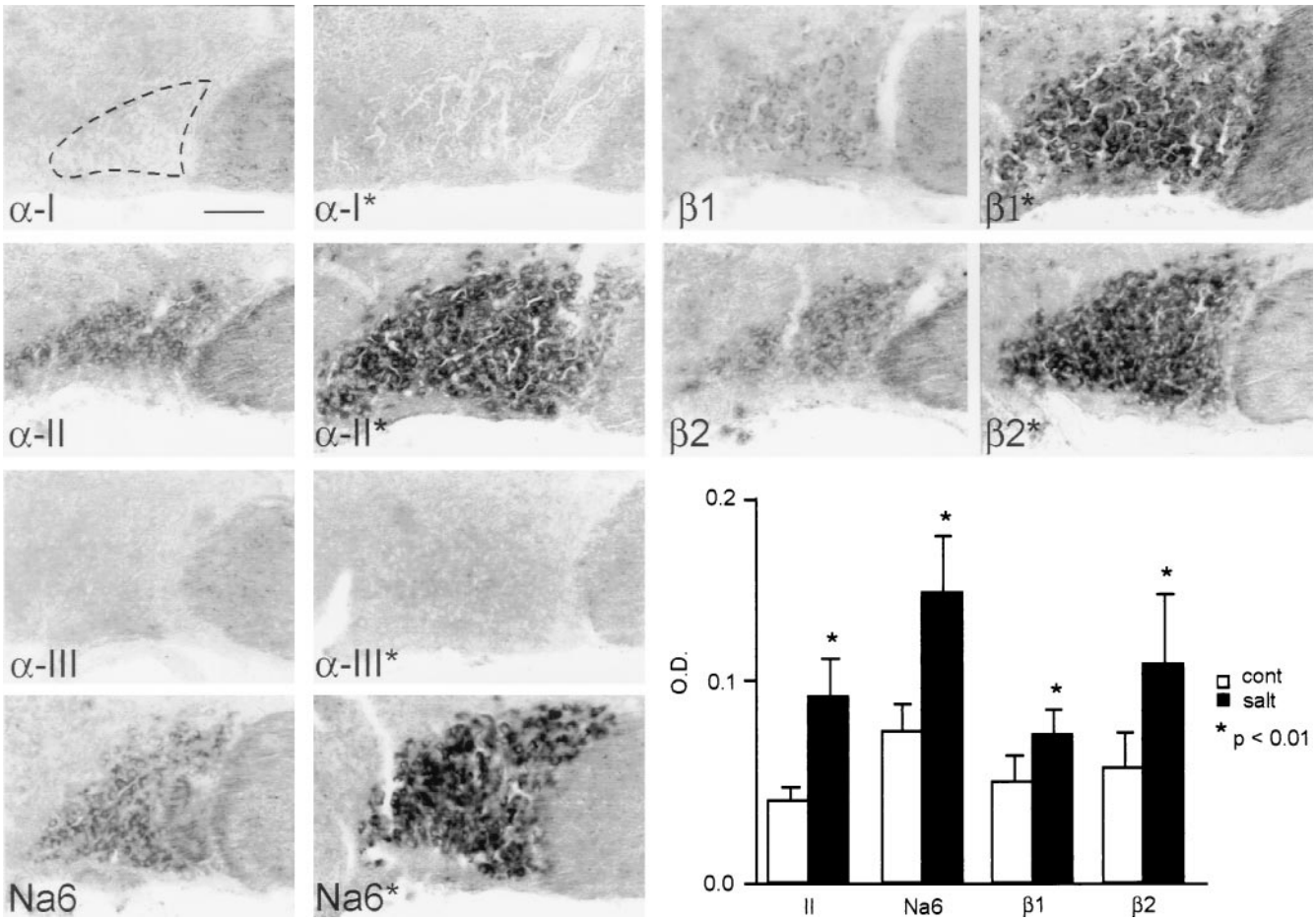

FIG. 2. *In situ* hybridization with subtype-specific riboprobes for Na^+ channel subunits α-I, α-II, α-III, Na6, β1, and β2 in the SON. α-I and α-III mRNA are not detectable. Low levels of α-II, Na6, β1, and β2 mRNA are present in the control SON (no asterisks), and there is a distinct up-regulation of each of these transcripts after salt-loading (asterisks). The fields shown were scanned from micrographs and digitally enhanced to illustrate the up-regulation of specific transcripts, but they do not illustrate the quantitative magnitudes of the changes. Optical densities from unenhanced micrographs (histogram, *Lower Right*) provide a quantitative measure of mRNA levels and show significant changes for α-II, Na6, β1, and β2 transcripts in salt-loaded rats. (Bar = 100 μm.)

There was distinct up-regulation of α-II, Na6, β1, and β2 mRNA levels, but not of α-I or α-III mRNA, in salt-loaded rats (Fig. 2), which was reflected by significant increases in optical density (histogram in Fig. 2). In addition to an increase in optical density, there was a significant increase in the area of SON expressing each of these transcripts (Fig. 2), because of increased cell sizes, as previously reported (29) in salt-loaded rats. Thus expression of specific Na^+ channel transcripts in MNCs was increased by salt-loading.

To determine whether the changes in Na^+ channel mRNA in the salt-loaded SON were paralleled by increases in Na^+ channel protein, we used SP20 antibody, which recognizes a conserved region in Na^+ channels (23), for immunocytochemistry and immunoblot analysis. Immunoreactivity in the SON was distinctly increased in salt-loaded rats (Fig. 3 *A* and *B*). In contrast, we did not detect differences in immunoreactivity of the median eminence or posterior pituitary, the sites of the axons and terminals of the SON MNCs (data not shown).

To further substantiate the effect of salt-loading on Na^+ channel expression, we performed Western blot analysis with SP20 antibody, using membrane preparations from the SON and from the site of termination of MNC axons, the posterior pituitary (Fig. 3*C*). In all lanes, a band of about 230 kDa, consistent with that previously reported (23), was present. Additional minor bands at ≈170 kDa may represent channel precursors or breakdown products. The 230-kDa immunoreactive band was stained more densely in the salt-loaded SON than in the control SON. The 230-kDa band from salt-loaded posterior pituitary gland was also denser than the control, but the difference was less pronounced. These immunoblots confirm and extend the results of SP20 immunocytochemistry in showing an increase in Na^+ channel protein in the salt-loaded SON and posterior pituitary.

These results show that the transcription of Na^+ channel mRNA is up-regulated in the salt-loaded SON and suggest that this up-regulation results in increased synthesis of Na^+ channel protein in these cells. To determine whether these changes result in increased incorporation of functional Na^+ channels in the membranes of these cells, we dissociated MNCs and carried out patch-clamp studies. MNC neurons were rapidly isolated from control rats ($n = 6$) and salt-loaded rats ($n = 6$). Both groups (Table 1) expressed fast, TTX-sensitive, sodium currents, but the peak sodium current amplitude (measured at 0 mV from a −130 mV holding potential) was 60% larger for MNC neurons isolated from the salt-loaded SON neurons (Fig. 4*A*; 15.8 ± 1.1 nA for control, $n = 44$; 25.3 ± 2.1 nA for salt-loaded, $n = 45$; $P < 0.001$). However, because the MNC neurons also exhibited a significant increase in soma size (measured by cell capacitance; 16.2 ± 0.4 pF control, 21.5 ± 0.8 pF salt-loaded; $P < 0.001$), peak current density (peak current amplitude divided by cell capacitance) was only 20% larger in freshly isolated salt-loaded MNC neurons. The voltage dependence of activation and steady-state inactivation were shifted about −6 mV for salt-loaded neurons compared with control neurons (Fig. 4*B*).

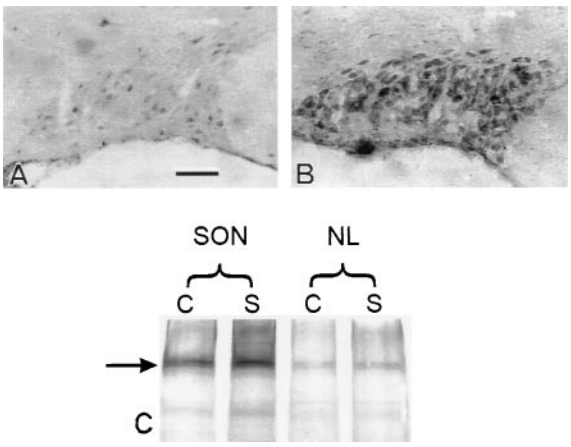

FIG. 3. Sodium channel immunoreactivity with SP20 antibody is increased in the SON of salt-loaded rats (*B*) compared with controls (*A*). Immunoblotting (*C*) shows a 230-kDa band (arrow) that is denser in the salt-loaded (S) SON than in the control (C) SON. There is a less pronounced increase in density of this band in the salt-loaded pituitary neural lobe (NL). (Bar = 100 μm.)

Because persistent sodium currents might contribute to the intrinsic burst activity of MNC neurons, we also examined sodium currents elicited with slow ramp depolarizations (0.23 mV/ms) in control and salt-loaded neurons. While TTX-sensitive sodium currents that activated near threshold (i.e., at potentials from −65 to −55 mV) were recorded in both groups, the salt-loaded neurons exhibited significantly ($P < 0.005$) larger threshold ramp currents (Fig. 4*C*). Because slow closed-state inactivation of sodium channels can underlie ramp currents (30), we examined the kinetics of inactivation at −80 mV. Both the development of inactivation and recovery from inactivation were significantly slower in salt-loaded neurons (Table 1), suggesting that the increased ramp currents in salt-loaded neurons arise at least in part from an increase in sodium channels with slow closed-state inactivation. The maximum ramp current amplitude was doubled (Table 1) and the ramp current density was ≈50% larger in the salt-loaded neurons (Fig. 4*D*). Thus, the peak and ramp currents were both increased after salt-loading, but to significantly different degrees. These results show that the functional properties of the sodium currents in salt-loaded SON neurons differ from those in control neurons in several ways. Because ramp currents activate at potentials close to threshold, these changes are expected to have an impact on the excitability of MNCs.

DISCUSSION

Our observations indicate that two Na^+ channel α subunits, α-II and Na6, are coexpressed in most MNCs in the SON. Two separable components of the Na^+ current have been identified in these cells, with transient and persistent kinetics (9, 25). In cerebellar Purkinje cells, which also express two Na^+ channel transcripts, Na6 appears to produce a persistent sodium current and α-I appears to produce a transient current (31). Ramp currents in Purkinje cells, similar to those that we evoked in MNCs, are produced by Na6 channels (32).

Our results demonstrate an up-regulation of mRNA for two Na^+ channel α subunits (α-II and Na6) and both β subunits (β1

Table 1. Properties of Na^+ channels

Measurement	Control	Salt-loaded	*P*
Cell capacitance, pF	16.2 ± 0.4	21.5 ± 0.8	<0.001
Transient current			
Peak amplitude, nA	15.8 ± 1.1	25.3 ± 2.1	<0.001
Density, pA/pF	989 ± 70	1206 ± 95	0.09
	$n = 44$	$n = 45$	
$V_{1/2}$ activation, mV	−28.5 ± 1.4	−34.4 ± 1.2	<0.005
$V_{1/2}$ inactivation, mV	−62.9 ± 1.3	−68.6 ± 1.4	<0.01
	$n = 17$	$n = 17$	
Inactivation kinetics			
Recovery at			
−80 mV, ms	13.6 ± 0.7	19.6 ± 1.7	<0.005
Development at			
−80 mV, ms	28.8 ± 2.2	37.7 ± 3.6	<0.05
	$n = 33$	$n = 30$	
Ramp current			
Amplitude, pA	190.3 ± 17	396.2 ± 50	<0.001
Density, pA/pF	12.0 ± 1.0	19.5 ± 2.3	<0.005
	$n = 34$	$n = 29$	

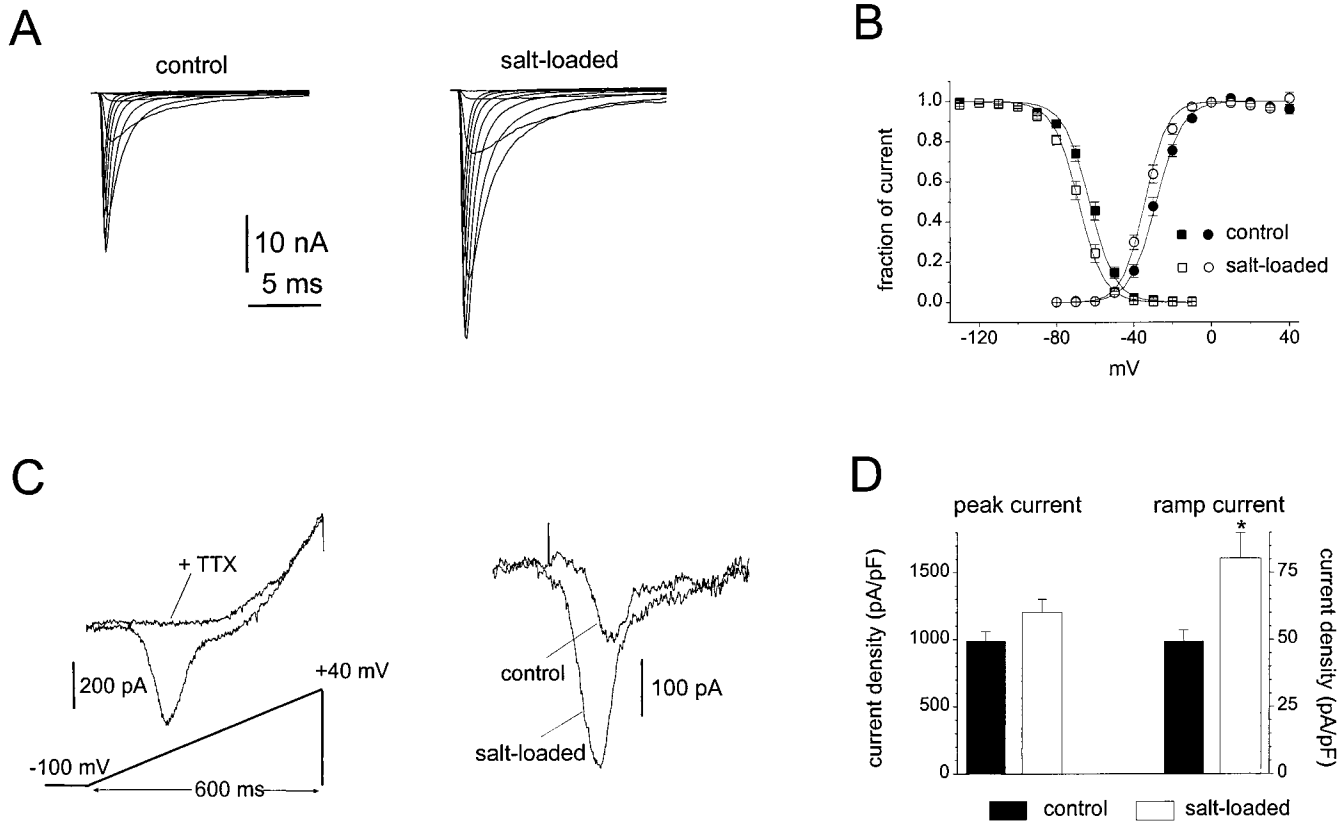

FIG. 4. Comparison of Na^+ currents in control and salt-loaded SON neurons. (*A*) Family of traces from representative SON neurons freshly isolated from control (*Left*) or salt-loaded (*Right*) rats. The currents were elicited by 40-ms test pulses to various potentials from −60 to 30 mV. Cells were held at −100 mV. (*B*) Normalized activation (circles) and steady-state inactivation (squares) data for control (filled symbols; $n = 17$) and salt-loaded (open symbols; $n = 17$) neurons. Curves through the points are fits to Boltzmann functions. For activation the $V_{1/2}$ and k values were −28.5 ± 1.4 and 6.7 ± 0.3 mV for control MNCs and −34.4 ± 1.2 and 5.8 ± 0.2 mV for salt-loaded MNCs. For inactivation the $V_{1/2}$ and k values were −62.9 ± 1.3 and 6.6 ± 0.2 mV for control MNCs and −68.6 ± 1.4 and 6.5 ± 0.2 mV for salt-loaded MNCs. Steady-state inactivation was measured with 500-ms inactivating prepulses. Cells were held at prepulse potentials over the range of −130 to −10 mV prior to a test pulse to 0 mV for 20 ms. Error bars indicate SE. (*C*) Ramp currents are elicited in MNCs by slow voltage ramps (600-ms voltage ramp extending from −100 to +40 mV). *Left* shows the ramp current in a salt-loaded MNC before and after the addition of 250 nM TTX to the extracellular solution. TTX blocks the ramp current. *Right* shows the TTX-sensitive ramp currents in representative control and salt-loaded MNCs. Leak currents recorded after application of 250 nM TTX were subtracted. (*D*) The peak and ramp current densities (estimated by dividing the maximum currents by the cell capacitance) are larger in salt-loaded neurons ($n = 29$) than in control neurons ($n = 34$); note that the increase is proportionately greater for the ramp currents. Error bars indicate SE, and the ∗ indicates $P < 0.005$.

and β2), and show increased levels of Na^+ channel protein and Na^+ current, in MNCs in the SON of salt-loaded rats. These results suggest that MNCs insert additional Na^+ channels, including auxiliary β subunits (33–35) in their membranes in response to osmotic changes. Peak sodium current amplitudes in salt-loaded MNCs were increased from 15.8 ± 1.1 nA to 25.3 ± 2.3 nA, while peak sodium current densities were increased by a smaller fraction (1,206 ± 95 pA/pF, salt-loaded; 989 ± 70 pA/pF, controls). This is probably due to the increase in cell size within the SON that occurs in salt-loaded animals (29). The increase in SP20 immunoreactivity within the salt-loaded SON, in the context of the relatively small increase in sodium current density (which provides a measure of average sodium channel density over the cell body, assuming a relatively uniform distribution of channels), might be interpreted as suggesting that additional Na^+ channels may have been added in a nonuniform pattern, clustered close to action potential trigger zones or other critical regions. Increased SP20 immunoreactivity within the salt-loaded SON, however, is also consistent with the alternative possibility of an increased pool of intracellular channels or channel precursors. This intracellular pool could serve to maintain Na^+ channel densities, possibly in the context of activity-related turn-over of channels (36–38), so as to maintain an appropriate level of electrogenic tuning. The increase in the ramp currents (Fig. 4 *C* and *D*), however, was greater than that of peak transient Na^+ current. This difference may be functionally important because noninactivating and slowly inactivating Na^+ channels, which produce ramp currents, can amplify generator and postsynaptic potentials and can contribute to the generation of tonic and phasic burst patterns in neurons (39–44).

Insertion of Na^+ channels in the membrane of MNCs may poise them to respond to changes in their input. MNCs release vasopressin [and oxytocin (45, 46)] from their terminals in response to osmotic stimulation. This neuropeptide release is related to the frequency of action potentials, which are known to be Na^+ dependent and TTX sensitive (6, 9) in these cells. Thus the expression of Na^+ channels may effect the burst threshold and contribute to the synaptically driven (21) as well as the endogenous component of the response to osmotic changes in these cells. Interestingly, there is a continued increase in the firing rate within bursts, from day to day, that is observed in phasic SON MNCs during a 5-day period of water deprivation (47).

Our results may have implications for neuronal cell types other than hypothalamic neurons. Persistent Na^+ channels contribute to oscillatory bursting behavior in a number of types of neurons (48–53). Electrical activity, cAMP, and cytosolic calcium levels regulate Na^+ channel α subunit expression in muscle (54) and neural cells (55–57). There is evidence for

plasticity in expression of other ion channels, including K^+ and Ca^{2+} channels that also contribute to neuronal excitability (58, 59). It is thus possible that expression of voltage-sensitive channels contributing to excitability is altered in neuronal cell types outside of the hypothalamus in response to changes in their input.

We have demonstrated that, in response to external stimuli, SON neurons respond not only by altering their firing patterns but also by selectively activating specific Na^+ channel genes and deploying additional functional channels so as to change the electrogenic properties of their membrane. Thus, these cells not only integrate incoming signals (generator potentials, postsynaptic potentials) so as to produce different patterns of electrical activity in response to changes in their environment but also rebuild the electrogenic machinery that integrates these signals and generates electrical activity. This molecular and functional remodeling may provide a novel mechanism that underlies state-dependent changes in the input–output functions of neurons.

We thank W. A. Catterall and R. Westenbroek for the gift of SP-20 antibody. This work was supported, in part, by the Medical Research Service, Department of Veterans Affairs, and by Grant RG-1912 from the National Multiple Sclerosis Society. M.T. was supported by Kyoto Prefectural University of Medicine. T.R.C. was supported by a fellowship from the Spinal Cord Research Foundation. K.I. was supported by a Multiple Sclerosis Research Fellowship from the Eastern Paralyzed Veterans Association.

1. Dreifuss, J. J., Kalnins, I., Kelly, J. S. & Ruf, K. B. (1971) *J. Physiol. (London)* **215,** 805–817.
2. Dyball, R. E. J. & Pountney, P. S. (1973) *J. Endocrinol.* **56,** 91–98.
3. Walters, J. K. & Hatton, G. I. (1974) *Physiol. Behav.* **13,** 661–667.
4. Arnauld, E., Dufy, B. & Vincent, J.-D. (1975) *Brain Res.* **100,** 315–325.
5. Mason, W. T. (1980) *Nature (London)* **287,** 154–157.
6. Andrew, R. D. & Dudek, F. E. (1983) *Science* **221,** 1050–1052.
7. Cobbett, P. & Mason, W. T. (1987) *Brain Res.* **409,** 175–180.
8. Inenaga, K., Nagatomo, T., Kannan, H. & Yamashita, H. (1993) *J. Physiol. (London)* **465,** 289–301.
9. Li, Z. & Hatton, G. I. (1996) *J. Physiol. (London)* **496,** 379–394.
10. Akopian, A. N., Sivilotti, L., Wood, J. N. (1996) *Nature (London)* **379,** 258–262.
11. Black, J. A., Dib-Hajj, S., McNabola, K., Jeste, J. Rizzo, M. A., Kocsis, J. D. & Waxman, S. G. (1996) *Mol. Brain Res.* **43,** 117–131.
12. Kayano, T., Noda, M., Flockerzi, V., Takahashi, H. & Numa, S. (1988) *FEBS Lett.* **228,** 187–194.
13. Noda, M., Ikeda, T., Kayano, T., Suzuki, H., Takeshima, I. I., Kurasaki, M. & Numa, S. (1986) *Nature (London)* **320,** 188–192.
14. Sangameswaran, L., Delgado, S. G., Fish, L. M., Koch, B. D., Jakeman, L. B., Stewart, G. R., Sze, P., Hunter, J. C., Eglen, R. M. & Herman, R. C. (1996) *J. Biol. Chem.* **271,** 5953–5956.
15. Schaller, K. L., Krzemien, D. M., Yarowsky, P. J., Krueger, B. K. & Caldwell, J. H. (1995) *J. Neurosci.* **15,** 3231–3242.
16. Toledo-Aral, J. J., Moss, B. L., He, Z.-J., Koszowski, A. G., Whisenand, T., Levinson, S. R., Wolf, J. J., Silos-Santiago, I., Halegoua, S. & Mandel, G. (1997) *Proc. Natl. Acad. Sci. USA* **94,** 1527–1532.
17. Dib-Hajj, S. D., Tyrrell, L., Black J. A. & Waxman, S. G. (1998) *Proc. Natl. Acad. Sci. USA* **95,** 8963–8968.
18. Hatton, G. I. (1982) *J. Physiol. (London)* **327,** 273–284.
19. Andrew, R. D. & Dudek, F. E. (1984) *J. Neurophysiol.* **51,** 552–566.
20. Ollet, S. H. R. & Bourque, C. W. (1993) *Nature (London)* **364,** 341–343.
21. Richard, D., Bourque, C. W. (1992) *Neuroendocrinology* **55,** 609–611.
22. Tanaka, M., Matsuda, T., Shigeyoshi, Y., Ibata, Y. & Okamura, H. (1997) *J. Histochem. Cytochem.* **45,** 1231–1237.
23. Westenbroek, R. E., Merrick, D. K. & Catterall, W. A. (1989) *Neuron* **3,** 695–704.
24. Hartshorne, R. P. & Catterall, W. A. (1984) *J. Biol. Chem.* **259,** 1667–1675.
25. Widmer, H., Amerdeil, H., Fontanaud, P. & Desarmenien, M. G. (1997) *J. Neurophysiol.* **77,** 260–271.
26. Jones, C. W. & Pickering, B. T. (1969) *J. Physiol. (London)* **203,** 449–458.
27. Balment, R. J., Brimble, M. J. & Forsling, M. L. (1980) *J. Physiol. (London)* **308,** 439–449.
28. Dogterom, J., Van Wimersma Greidanus, B. & Swaab, D. F. (1977) *Neuroendocrinology* **24,** 108–118.
29. Hatton, G. I. & Walters, J. K. (1973) *Brain Res.* **59,** 137–154.
30. Cummins, T. R., Howe, J. R. & Waxman, S. G. (1998) *J. Neurosci.* **18,** 9607–9619.
31. Vega-Saenz de Miera, E., Rudy, B., Sugimori, M. & Llinás, R. (1997) *Proc. Natl. Acad. Sci. USA* **94,** 7059–7064.
32. Raman, I. M., Sprunger, L. K., Meisler, M. K. & Bean, B. P. (1997) *Neuron* **19,** 881–891.
33. Isom, L. L., De Jongh, K. S., Patton, D. E., Reber, B. F. X., Offord, J., Charbonneau, H., Walsh, K., Goldin, A. L. & Catterall, W. A. (1992) *Science* **256,** 839–842.
34. Isom, L. L., Ragsdale, D. S., De Jongh, K. S., Westenbroek, R. E., Reber, B. F. X., Scheuer, T. & Catterall, W. A. (1995) *Cell* **83,** 433–442.
35. Isom, L. L., De Jongh, K. S. & Catterall, W. A. (1994) *Neuron* **12,** 1183–1194.
36. Waxman, S. G. (1997) *Adv. Neurol.* **73,** 109–121.
37. Dargent, B., Paillart, C., Carlier, E., Alcaraz, G., Martin-Eauclaire, M. F. & Couraud, F. (1994) *Neuron* **13,** 683–690.
38. Wonderlin, W. F. & French, R. J. (1991) *Proc. Natl. Acad. Sci. USA* **88,** 4391–4395.
39. Stafstrom, C. E., Schwindt, P. C., Flatman, J. A. & Crill, W. E. (1984) *J. Neurophysiol.* **52,** 244–263.
40. Huguenand, J. R., Hammill, O. P. & Prince, D. A. (1989) *Proc. Natl. Acad. Sci. USA* **86,** 2473–2477.
41. Matzner, O. & Devor, M. (1992) *Brain Res.* **597,** 92–98.
42. Lipowsky, R., Gillessen, T. & Alzheimer, C. (1996) *J. Neurophysiol.* **76,** 2181–2191.
43. Stuart, G. & Sakmann, B. (1995) *Neuron* **15,** 1065–1076.
44. Pennartz, C. M., Bierlaagh, M. A. & Geurtsen, A. M. S. (1997) *J. Neurophysiol.* **78,** 1811–1825.
45. Franco-Bourland, R. E. & Fernstrom, J. D. (1981) *Endocrinology* **109,** 1097–1102.
46. Van Tol, H. H. M., Voorhuis, O. T. A. M. & Burbach, J. P. H. (1987) *Endocrinology* **120,** 71–76.
47. Walters, H. K. & Hatton, G. I. (1974) *Physiol. Behav.* **13,** 661–667.
48. Alonso, A., Llinas, R. R. (1989) *Nature (London)* **342,** 175–177.
49. Llinás, R. R., Grace, A. A. & Yarom, Y. (1991) *Proc. Natl. Acad. Sci. USA* **88,** 897–901.
50. Fleidervish, I. A., Friedman, A. & Gutnick, M. J. (1996) *J. Physiol. (London)* **493,** 83–97.
51. Jahnsen, H. & Llinas, R. (1984) *J. Physiol. (London)* **349,** 227–247.
52. Parri, H. & Crunelli, V. (1998) *J. Neurosci.* **18,** 854–867.
53. Stafstrom, C. E., Schwindt, P. C., Chubb, M. C. & Crill, W. E. (1985) *J. Neurophysiol.* **53,** 153–170.
54. Offord, J. & Catterall, W. A. (1989) *Neuron* **2,** 1447–1452.
55. Hirsh, J. K. & Quandt, F. N. (1996) *Brain Res.* **706,** 343–346.
56. Sashihara, S., Waxman, S. G. & Greer, C. A. (1997) *NeuroReport* **8,** 1289–1293.
57. Oh, Y., Lee, Y.-J. & Waxman, S. G. (1997) *Neurosci. Lett.* **234,** 107–110.
58. Wu, R.-L. & Barish, M. E. (1994) *J. Neurosci.* **14,** 1677–1687.
59. O'Dowd, D. K., Ribera, A. B. & Spitzer, N. C. (1988) *J. Neurosci.* **8,** 792–805.